ORIGINAL ARTICLE

JBMR®

Bone Fracture Toughness and Strength Correlate With Collagen Cross-Link Maturity in a Dose-Controlled Lathyrism Mouse Model

Erin MB McNerny,[1] Bo Gong,[2] Michael D Morris,[2] and David H Kohn[1,3]

[1]Department of Biomedical Engineering, College of Engineering and Medical School, University of Michigan, Ann Arbor, MI, USA
[2]Department of Chemistry, College of Literature, Science and the Arts, University of Michigan, Ann Arbor, MI, USA
[3]Department of Biologic and Materials Sciences, School of Dentistry, University of Michigan, Ann Arbor, MI, USA

ABSTRACT

Collagen cross-linking is altered in many diseases of bone, and enzymatic collagen cross-links are important to bone quality, as evidenced by losses of strength after lysyl oxidase inhibition (lathyrism). We hypothesized that cross-links also contribute directly to bone fracture toughness. A mouse model of lathyrism using subcutaneous injection of up to 500 mg/kg β-aminopropionitrile (BAPN) was developed and characterized (60 animals across 4 dosage groups). Three weeks of 150 or 350 mg/kg BAPN treatment in young, growing mice significantly reduced cortical bone fracture toughness, strength, and pyridinoline cross-link content. Ratios reflecting relative cross-link maturity were positive regressors of fracture toughness (HP/[DHLNL + HLNL] $r^2 = 0.208$, $p < 0.05$; [HP + LP]/[DHNL + HLNL] $r^2 = 0.196$, $p < 0.1$), whereas quantities of mature pyridinoline cross-links were significant positive regressors of tissue strength (lysyl pyridinoline $r^2 = 0.159$, $p = 0.014$; hydroxylysyl pyridinoline $r^2 = 0.112$, $p < 0.05$). Immature and pyrrole cross-links, which were not significantly reduced by BAPN, did not correlate with mechanical properties. The effect of BAPN treatment on mechanical properties was dose specific, with the greatest impact found at the intermediate (350 mg/kg) dose. Calcein labeling was used to define locations of new bone formation, allowing for the identification of regions of normally cross-linked (preexisting) and BAPN-treated (newly formed, cross-link-deficient) bone. Raman spectroscopy revealed spatial differences attributable to relative tissue age and effects of cross-link inhibition. Newly deposited tissues had lower mineral/matrix, carbonate/phosphate, and Amide I cross-link (matrix maturity) ratios compared with preexisting tissues. BAPN treatment did not affect mineral measures but significantly increased the cross-link (matrix maturity) ratio compared with newly formed control tissue. Our study reveals that spatially localized effects of short-term BAPN cross-link inhibition can alter the whole-bone collagen cross-link profile to a measureable degree, and this cross-link profile correlates with bone fracture toughness and strength. Thus, cross-link profile perturbations associated with bone disease may provide insight into bone mechanical quality and fracture risk. © 2014 American Society for Bone and Mineral Research.

KEY WORDS: COLLAGEN CROSS-LINKS; FRACTURE TOUGHNESS; BIOMECHANICS; β-AMINOPROPIONITRILE (BAPN); RAMAN SPECTROSCOPY

Introduction

Resistance to fracture is dependent not only on the quantity and distribution of bone but also on the quality of the bone material.[1–3] As a hierarchical composite primarily composed of mineral and Type I collagen matrix, the strength and toughness of bone tissue are derived from its components' individual properties, as well as their interfaces and arrangements at multiple length scales. A stiff bone is desirable as a skeletal support, but tough bone is necessary to resist fracture.[4–6] Toughness is supplied primarily by the organic matrix,[3,7,8] and the task of stabilizing this polymeric network rests on a collection of covalent collagen cross-links.[9–12]

Numerous species of collagen cross-links have been characterized.[13–17] The conversion of collagen telopeptide lysines to allysines by the extracellular enzyme lysyl oxidase (LOX) is required for the formation of enzymatically controlled cross-links during tissue development.[18] LOX-produced allysines react with helix (hydroxy)lysines on neighboring collagen molecules to form immature divalent cross-links, quantified as their reduced forms dihydroxylysinorleucine (DHLNL) and hydroxylysinorleucine (HLNL). A fraction of these cross-links will subsequently mature to trivalent forms, known to include both the pyridinolines (hydroxylysylpyridinoline [HP] and lysylpyridinoline [LP]) and pyrroles. Advanced glycation endproduct (AGE) cross-links, such as pentosidine (PEN), form independently of enzyme activity in the presence of sugars with net accumulation determined by their rate of formation and removal via tissue turnover. Shifts in cross-link profile occur in many bone pathologies and with aging,[19–22] and understanding which of these changes are significant to bone fracture resistance is critical for developing and evaluating therapies for fracture prevention and disease management.

Received in original form May 9, 2014; revised form August 28, 2014; accepted September 5, 2014. Accepted manuscript online September 11, 2014.
Address correspondence to: David H Kohn, PhD, 1011 North University Avenue, Ann Arbor, MI 48109-1078, USA. E-mail: dhkohn@umich.edu
Additional Supporting Information may be found in the online version of this article.

Journal of Bone and Mineral Research, Vol. 30, No. 3, March 2015, pp 446–455
DOI: 10.1002/jbmr.2356

There are many reports of enzymatic and AGE cross-links differing in their contribution to bone mechanics,[1,19,21,23,24] but a full characterization of cross-link profile (eg, immature versus mature, hydroxylation level, enzymatic versus AGE) with direct correlations to tissue fracture toughness is unknown. Inhibition of lysyl oxidase by treatment with β-aminopropionitrile (BAPN), known as lathyrism, inhibits enzymatic cross-link formation in forming collagen and reduces bone strength in vivo.[25–27] The majority of studies investigating the effects of BAPN on bone use animal models no smaller than rats.[27–30] Most commonly, BAPN is administered through diet or ingested fluids, which make the dose difficult to control.[25,27,30,31] Subcutaneous BAPN injection of mice was chosen in this study to allow for dosage control of cross-link inhibition in an inexpensive animal model. Enzymatic cross-linking occurs primarily during tissue formation. Thus, young, growing mice were chosen so that significant quantities of cross-link–deficient tissue were deposited during the course of BAPN exposure. Cross-link profile (DHLNL, HLNL, HP, LP, Pyrrole, and PEN), whole-bone mechanical properties, fracture toughness, and localized matrix composition were measured on hind limb bones from mice treated with 0 to 500 mg BAPN/kg body weight from 5 to 8 weeks of age. We hypothesized that shifts in cross-link profile after BAPN treatment would be dose dependent and would specifically correlate with resulting reductions in bone fracture toughness and strength.

Materials and Methods

Animals and BAPN treatment

All animal procedures were performed at the University of Michigan with University Committee on Use and Care of Animals (UCUCA) approval. Sixty male C57Bl6 mice (Charles River Laboratories, Wilmington, MA, USA) were weight-matched into 4 experimental groups 2 days before the start of the experiment. Animals were group housed in standard cages with free access to standard chow, water, and cage activity. All mice underwent 3 weeks of treatment beginning when mice reached 5 weeks of age. Treatment consisted of daily subcutaneous injections of phosphate buffered saline (PBS) containing 0, 150, 350, or 500 mg/kg BAPN (β-aminopropionitrile fumarate, Sigma-Aldrich, St. Louis, MO, USA). Mice were weighed and dosages adjusted every 3 days during the course of the 21-day experiment. On experiment days 2 and 16, mice received 15 mg/kg calcein (Sigma) by intraperitoneal injection. Mice were euthanized by CO_2 inhalation on day 22 at 8 weeks of age. Femora and tibias were immediately harvested, cleaned of soft tissue, wrapped in calcium-buffered PBS (Ca-PBS)–soaked gauze and frozen until use.

μCT

Whole left tibias and femora ($n = 15$/group) were scanned while submerged in Ca-PBS using an eXplore Locus SP scanner (GE Healthcare Pre-Clinical Imaging, London, Canada) at a voxel size of 18 μm^3 (80 kVp, 80 μA, 1600 ms, 0.508 mm Al filter).[32] Calibration of the scanner using an air/water/hydroxyapatite (HA) phantom was performed each day of scanning. Regions of interest were analyzed using a combination of GE MicroView software (reorientation, standard site selection, tissue mineral content [TMC] and tissue mineral density [TMD]) and custom-written MATLAB scripts (quantification of cortical geometry). Scans were reoriented to match the alignment of each bone in silico with its eventual alignment during mechanical testing. A five-slice-thick standard site was taken from each reoriented tibia at the point 23.5% of the distance from the tibia-fibula junction to the proximal end of the tibia, closely corresponding to the center of the 3 mm mechanical testing span for all bones. Thus, the cortical site analyzed was reproducible from bone to bone and appropriate for calculating tissue level properties from four-point testing data using classic beam theory. For the femur, a five-slice standard site was located at the site 48% of its length as measured from the distal condyle. TMC and TMD were measured for both the femur and tibia using a fixed threshold of 2000 Hounsfield Units.

Four-point bending

After μCT scanning, left tibias ($n = 15$/group) were tested in four-point bending on an eXpert 450 Universal Testing Machine (Admet, Norwood, MA, USA) as previously described.[33] Briefly, bones were oriented with the medial surface in tension and loaded at a displacement rate of 0.025 mm/s. Bones were hydrated with Ca-PBS at all times. Load and displacement (structural-level) data were recorded and tissue stress and strain were estimated from the structural-level data using beam theory and the tibia standard site cross-sectional geometry measured by μCT. Whole-bone (load, displacement) and estimated tissue level (stress, strain) properties were quantified at the yield and ultimate points. Yield was defined using the 0.2% strain offset method. Whole-bone stiffness and estimated tissue elastic modulus were calculated by linear regression fitting of the linear-elastic pre-yield region. Pre-yield work and estimated pre-yield toughness (resilience) were calculated as the area under the load-displacement and stress-strain curves, respectively, up to the previously defined yield point.

Notched toughness testing

A notched toughness test was performed on the right femora.[34] A sharp notch was cut through the anterior surface of the mid-diaphysis using a razor blade lubricated with 1 μm diamond suspension (MetaDi Supreme, Buehler, Lake Bluff, IL, USA) and a custom-built jig. Razor cutting depth was controlled using a micrometer. Notched bones were tested to catastrophic failure in three-point bending at 0.001 mm/s. Load and deflection were recorded during each test. After fracture, bones were briefly soaked in diluted household bleach to remove marrow from the fracture surface and then dehydrated in a graded ethanol series. Fracture surfaces were imaged under back-scattering scanning electron microscopy (SEM, Hitachi S3200N, Hitachi, Tokyo, Japan) and analyzed using a custom MATLAB script to quantify bone geometry, half-notch and half-crack angles, and calculate maximum load ($K_{C.Max}$) and instability ($K_{C.Inst}$) toughness.[34] $K_{C.Max}$ was calculated using the ultimate force and half-notch angle. $K_{C.Inst}$ was calculated using the force at catastrophic fracture and instability half-crack angle. Notch and crack geometry met the assumptions of the thick-walled cylinder crack propagation model, with half-notch/crack angles less than 110°.[34] Sample sizes were 7 to 10 per group.

Collagen cross-link quantification

Left femora were used for collagen cross-link quantification ($n = 7$ to 11/group). Mature (HP, LP, and pyrrole), reduced immature (DHLNL and HLNL), and glycation (PEN) cross-links were all measured from the same sample and normalized to collagen content. Cortical diaphyses, flushed of marrow, were demineralized in 0.5M EDTA. After extensive washing, demineralized

samples were reacted with sodium borohydride to stabilize immature cross-links in preparation for acid hydrolysis.[35] Because pyrrole cross-links are neither reducible nor stable in strong acid, reduced samples were first digested with TPCK-treated trypsin in a shaking water bath at 37°C for 22 hours.[35] An aliquot of digest was used to quantify pyrrole content colorimetrically in a 384-well plate.[35] The remaining digest was mixed 1:1 with 12M HCl and hydrolyzed at 110°C for 12 hours. An aliquot of the resulting hydrolysate was used for hydroxyproline quantification to determine collagen content.[36] Another aliquot was mixed with an internal standard (Quidel, San Diego, CA, USA) and applied to an SPE column (Chromabond X-Links, Machery-Nagel, Germany) optimized for the purification of collagen cross-links from biological samples.[37] Cross-links and internal standard were eluted from the SPE column in 600 μL of 1% heptafluorobutyric acid (HFBA) in preparation for HPLC injection.

HP and LP were quantified using a commercially available standard (Quidel). Pentosidine was synthesized as polypentosidine, hydrolyzed, and purified as described.[38] Further purification on Chromabond Cross-links SPE columns and by HPLC peak fraction collection yielded a pentosidine standard that matched published absorption and fluorescence profiles.[39] The pentosidine standard was calibrated from its absorbance at 326 nm in 1 mM HCl.[40] Standards for DHLNL and HLNL were a generous gift from Simon Robins (University of Aberdeen).

All cross-links but the pyrroles were quantified using a binary pump Waters Breeze HPLC system (Waters Corp., Milford, MA, USA) fitted with a column heater (set to 30°C) and Waters 2475 fluorescence detector. Samples were separated on a Waters XBridge C18 column (3.5 mm, 4.6 × 150 mm). Buffer A consisted of 0.12% HFBA and buffer B consisted of 50% acetonitrile. The naturally fluorescent cross-links were quantified in a single injection by monitoring at 297 nm/395 nm (HP, LP) and 335 nm/385 nm (PEN) ex/em wavelengths (10 minutes 85% A, linear gradient 85% to 75% A over 30 minutes, 10 minutes 75% A). The reduced immature cross-links were quantified in a second injection with the addition of an o-phthalaldehyde (OPA) post-column reaction (isocratic, 85% A). OPA reagent (0.8 g OPA dissolved in 15 mL ethanol, added to 980 mL boric acid buffer [0.4 M, pH 10], 2 mL mercaptoethanol, and 1 g Brij-35) was delivered using a high-pressure syringe pump (Nexus 5000, Chemyx, Stafford, TX, USA) at a rate of 0.5 mL/min with fluorescence monitored at 350 nm/450 nm (ex/em).

Bone sectioning and Raman spectroscopy

Right tibias ($n = 5$ to 7/group) were dehydrated in a graded ethanol series, cleared with Clear-Rite 3 (Thermo Fisher Scientific, Pittsburgh, PA, USA), and infiltrated and embedded using Koldmount (SPI Supplies, West Chester, PA, USA). Sections ~150 μm thick were cut from the mid-diaphysis using a low-speed sectioning saw (Model 650; South Bay Technology, San Clemente, CA, USA). Sections were mounted on glass slides and hand ground and polished to a final thickness of 75 to 100 μm. Calcein labels were imaged on a Nikon E800 fluorescence light microscope equipped with an FITC filter and Photometrics Coolsnap monochrome camera (Photometrics, Tucson, AZ, USA).

Using a locally constructed Raman microscope as described in detail previously,[41] four spectra were collected from each anatomical direction by means of line-focused laser radiation (785 nm excitation). Calcein images were referenced to identify each Raman collection site as preexisting or new tissue, thus identifying tissue age (before or with treatment) (Supplemental Fig. S1). For all Raman spectra, both bone mineral and matrix-specific Raman bands were analyzed, and band intensities for calculating the ratios of carbonate/phosphate (1070 cm^{-1}/960 cm^{-1}) and mineral/matrix (phosphate/phenylalanine, 958 cm^{-1}/1001 cm^{-1}) were measured (GRAMS/AI software, Thermo Nicolet, Middleton, WI, USA). The intensities of the two major components of amide I band, identified as 1660 and 1683 cm^{-1}, were used to calculate the cross-link (matrix maturity) ratio. Data were averaged for each bone section or cell culture sample before calculating group means, thus group sample sizes reflect only independent biological replicates.

Cell culture

Because bone samples included tissue varying in treatment history and age, we used extracellular matrix produced by MC3T3-E1 cells to verify the effect of collagen cross-link deficiency on Raman signal. MC3T3-E1 cells were plated in osteogenic media at a density of 8400 cells/cm^2 in six-well plates. Media consisted of α-MEM supplemented with 10% fetal bovine serum, 1% pen-strep, 50 mg/L ascorbic acid, 10^{-8} M dexamethasone, 10 mM β-glycerophosphate, and, for BAPN-treated wells only, 1.6 mM BAPN.[42] After 2.5 weeks of culture, cell layers were scraped and immediately transferred to a sapphire disc in a minimal amount of media for Raman measurement. Spectra were collected from each sample with the laser focused within the globule of matrix. Raman parameters were the same as described for tissue sections.

Statistics

All statistical analysis was performed in IBM SPSS Statistics software (SPSS, Inc., Chicago, IL, USA). Results were checked for assumptions of normality (Shapiro-Wilk) and homogeneity of variance (Levene), and, when both assumptions were valid, ANOVA tests with Dunnett post hoc comparisons were used to check for significant effects of BAPN dose and specific differences between BAPN-treated groups and controls (0 mg/kg dose). These results are reported as the group mean ± the standard error of the mean. In cases where normality tests failed, the nonparametric Jonckheere-Terpstra (J-T) test for ordered alternatives was used to test for a dose effect of BAPN. For these cases, stepwise post hoc comparisons were used to test for specific group differences. Results for non-normally distributed measures are reported as group median and 95% confidence interval. For Raman data, a two-way repeated measures ANOVA was used to test for the effects of tissue age (within-subject repeated measure) and BAPN dose (between-subjects measure). A one-way ANOVA was also used to test the effect of BAPN dose within new tissue only. Stepwise multivariable linear regressions were performed with fracture toughness and estimated material mechanical properties as dependent variables and cross-link measures and TMD as independent variables. Measures of pre-yield toughness, pentosidine, and pyrrole were transformed as detailed in Table 2 before regression to meet normality assumptions. Only single-variable models were found to be significant, thus only single-variable regressions are presented. In all tests, $p < 0.05$ was considered significant. Values of $p < 0.10$ are noted as trends.

Results

BAPN treatment reduces mouse growth and tibia cortical size

Mice were weight-matched into 4 treatment groups 2 days before the start of treatment with group mean body weights of

Table 1. Mouse Body Weight and Tibia Cortical Geometry Measures

	BAPN dose (mg/kg body weight)								
	0		150		350		500		p Value*
Body weight									
Day-2 (g)	15.4	(14.7–15.9)	15.4	(14.6–16.0)	15.3	(14.3–16.0)	15.2	(14.6–16.0)	
Day 18 (g)	20.4[a]	(20.0–21.5)	20.8[a]	(20.3–21.8)	20.6[a]	(19.6–21.4)	19.1[b]	(18.5–20.3)	0.028
Day 22 (g)	21.5[a]	(20.1–22.2)	21.1[a]	(19.9–22.1)	20.5	(19.4–21.2)	19.9[b]	(18.9–20.9)	0.009
Tibia									
Length (mm)	16.70	(16.56–16.79)	16.81	(16.58–16.88)	16.76	(16.45–16.90)	16.61	(16.42–16.81)	
TMC (μg HA)	49.0[a]	(47.7–52.1)	46.7[a]	(44.9–51.1)	47.6	(45.5–49.7)	45.1[b]	(44.0–47.4)	0.011
Ct.Area (mm^2)	0.543[a]	(0.534–0.569)	0.532[a]	(0.495–0.579)	0.529	(0.503–0.550)	0.503[b]	(0.489–0.540)	0.013
Ct.Th (mm)	0.163	(0.160–0.175)	0.161	(0.154–0.178)	0.163	(0.154–0.172)	0.157	(0.150–0.164)	0.052
I_{AP} (mm^4)	0.051[a]	(0.046–0.054)	0.049[a]	(0.048–0.053)	0.046	(0.045–0.052)	0.044[b]	(0.040–0.049)	0.007
I_{ML} (mm^4)	0.070[a]	(0.065–0.081)	0.069	(0.059–0.078)	0.066	(0.057–0.077)	0.062[b]	(0.051–0.067)	0.038
AP.W (mm)	1.271	(1.219–1.351)	1.274	(1.193–1.343)	1.244	(1.194–1.317)	1.215	(1.154–1.267)	0.072
ML.W (mm)	1.137	(1.104–1.157)	1.143	(1.119–1.157)	1.127	(1.104–1.140)	1.121	(1.084–1.147)	0.099
AP/ML ratio	1.108	(1.063–1.174)	1.113	(1.075–1.139)	1.115	(1.049–1.158)	1.095	(1.047–1.150)	

Data presented as median (interquartile range).

TMC = tissue mineral content; HA = hydroxyapatite; Ct.Area = cortical area; Ct.Th = cortical thickness; I_{AP} = moment of inertia about anterior-posterior axis; I_{ML} = moment of inertia about medial-lateral axis; AP.W = anterior-posterior width; ML.W = medial-lateral width.

*Effect of BAPN tested using Jonckheere-Terpstra nonparametric test; post hoc differences indicated as [b]significantly different from [a]($p < 0.05$).

15.27 ± 0.25 g (mean ± SEM) (Table 1). Although all mice gained weight over the course of the 3-week experiment, the highest dose of BAPN significantly reduced growth, resulting in significant differences in body weight by day 18 of the experiment (J-T $p = 0.028$). At death, mice at the highest dose weighed 7.5% less than controls (J-T $p = 0.009$, post hoc $p < 0.05$).

Tibia cortical cross-sectional geometric measures were significantly reduced with BAPN treatment (Table 1). Tibia cross-sectional cortical area (Ct.Area) and TMC were significantly reduced with increasing BAPN dose (J-T, $p = 0.013$ and $p = 0.011$, respectively), as were the second moments of inertia about the anterior-posterior (I_{AP}) and medial-lateral axes (I_{ML}), indicating a reduction of the cross section's ability to resist bending in both the A-P and M-L directions (J-T, $p = 0.007$ and $p = 0.038$, respectively). BAPN treatment had no significant effects on femur cortical geometry (Supplemental Table S1). Although mean TMD for the tibia and femur were not different between BAPN groups, tibial TMD became more variable with BAPN treatment (Levene's homogeneity of variance test, $p < 0.05$) (Fig. 1).

BAPN treatment reduced pyridinoline cross-linking and cross-link maturity ratios

BAPN significantly reduced both species of pyridinoline cross-links compared with controls (Fig. 2*A*, ANOVA, HP: $p = 0.025$, LP: $p = 0.011$, (HP + LP): $p = 0.019$). Pyrroles were more abundant than the pyridinolines for all doses of BAPN (Fig. 2*A*, two-way ANOVA with cross-link measures treated as repeated measures, $p < 0.001$). However, no significant effect of BAPN dose on pyrrole content was measured (Fig. 2*A*). No differences in the immature cross-links DHLNL and HLNL (Fig. 2*B*) or pentosidine (Fig. 2*C*) with BAPN treatment were detected. Cross-link maturity ratios (Fig. 3) were significantly reduced with BAPN treatment when HP or (HP + LP) was used as the measure of mature cross-links. We also compared the proportions between the hydroxylated and nonhydroxylated forms of the pyridinolines and divalent cross-links (HP:LP and DHLNL:HLNL, respectively) but observed no significant changes with BAPN treatment (data not shown). There were no differences in the ratio of pyrroles to pyridinolines either (data not shown).

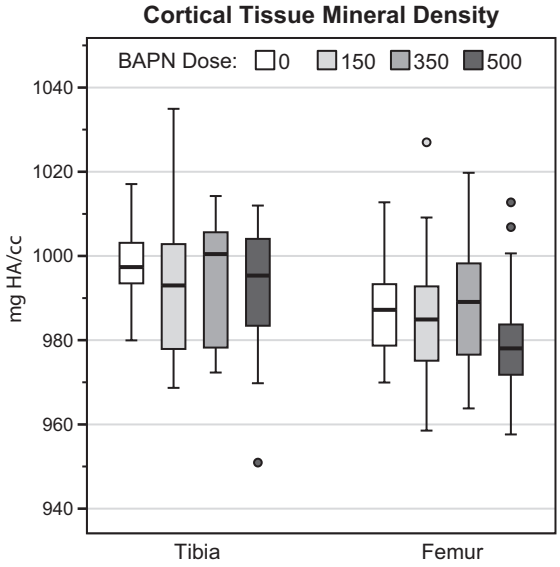

Fig. 1. Group distributions of TMD measured at the standard site are presented in a statistical boxplot. Black horizontal bars indicate group median, box ends indicate the 25th and 75th percentiles of the data, box height is the interquartile range (IQR) of the data, and whisker lines indicate the maximum and minimum values that are not outliers. Outliers are shown as individual dots. TMD was not significantly altered by dose for either bone, but tibia TMD variability was significantly increased by BAPN treatment, illustrated by the increased IQR in BAPN-treated groups (Levene's test for homogeneity of variance, $p = 0.026$).

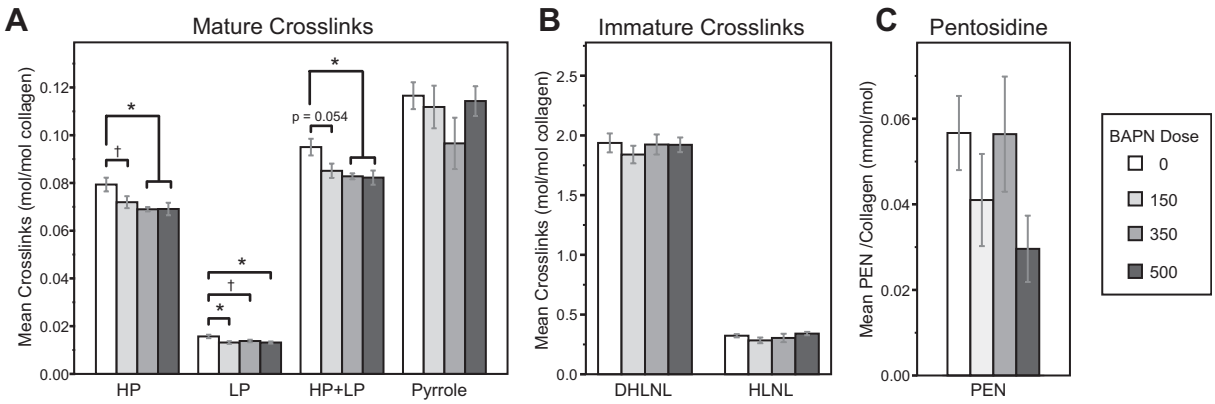

Fig. 2. Collagen cross-link quantification. (*A*) Pyridinolines were significantly reduced by BAPN treatment. HP was significantly less than controls for both the intermediate (350 mg/kg) and high (500 mg/kg) BAPN doses. LP was significantly lower than control for 150 and 500 doses of BAPN. Total pyridinolines (HP + LP) were significantly reduced by BAPN with significant post hoc differences found at the 350 and 500 mg/kg BAPN doses. Pyrrole cross-links were more abundant than the sum of the pyridinolines, but a significant effect of BAPN was not found for pyrrole cross-links. BAPN did not significantly affect immature (*B*) or pentosidine (*C*) cross-links. Post hoc: $^{*}p < 0.05$, $\dagger p < 0.10$.

Bone fracture toughness is reduced with intermediate doses of LOX inhibitor

Maximum load fracture toughness ($K_{C.Max}$) reflects the energy required for crack initiation and was significantly affected by BAPN treatment (Fig. 4, ANOVA $p = 0.010$). The 150 mg/kg ($p = 0.040$) and 350 mg/kg ($p = 0.019$) doses led to reductions in $K_{C.Max}$ of 15.5% and 18.2%, respectively. No difference was found between the 500 mg/kg dose and controls. Although the data suggest a reduction in instability toughness ($K_{C.Inst}$) at the 350 mg/kg dose, there was not a significant effect of BAPN dose (ANOVA $p = 0.408$).

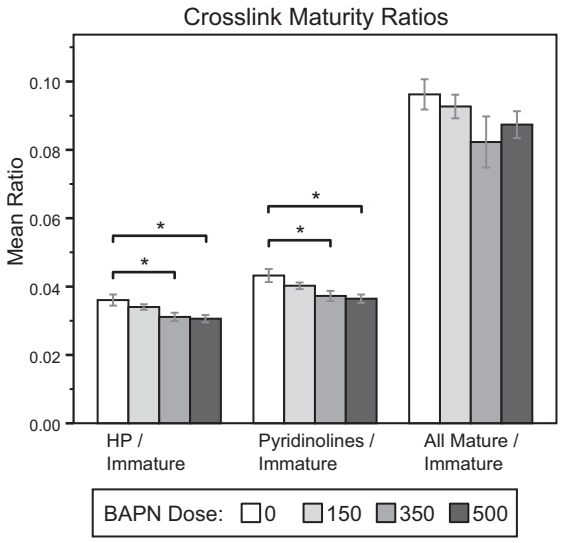

Fig. 3. Cross-link maturity. Relative cross-link maturity was significantly decreased with BAPN treatment when calculated using HP or (HP + LP) as the measure of mature cross-links, with 350 and 500 mg/kg dose groups significantly reduced compared with controls. $^{*}p < 0.05$.

Bone strength, but not stiffness, is reduced at both the structural and tissue levels with intermediate doses of BAPN

Significant reductions in structural strength occurred with BAPN treatment (Fig. 5*B*). Increasing BAPN dose reduced yield (J-T, $p = 0.054$) and ultimate (J-T, $p = 0.02$) strength (Fig. 5*B*). Estimated material properties (Fig. 5*D–F*) were also impacted by BAPN treatment, with significant reductions in yield (ANOVA,

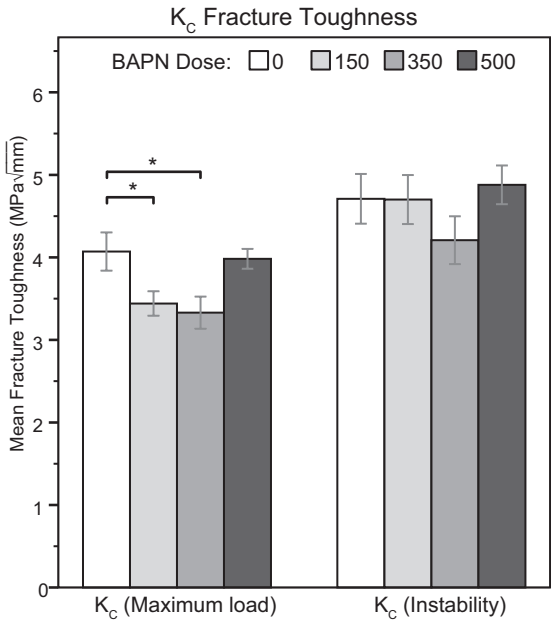

Fig. 4. K_C fracture toughness of the femur measured using a sharp-notched failure test. BAPN was a significant factor in maximum load toughness but not instability toughness. The greatest reductions in fracture toughness were found at the intermediate (350 mg/kg) BAPN dose. $^{*}p < 0.05$.

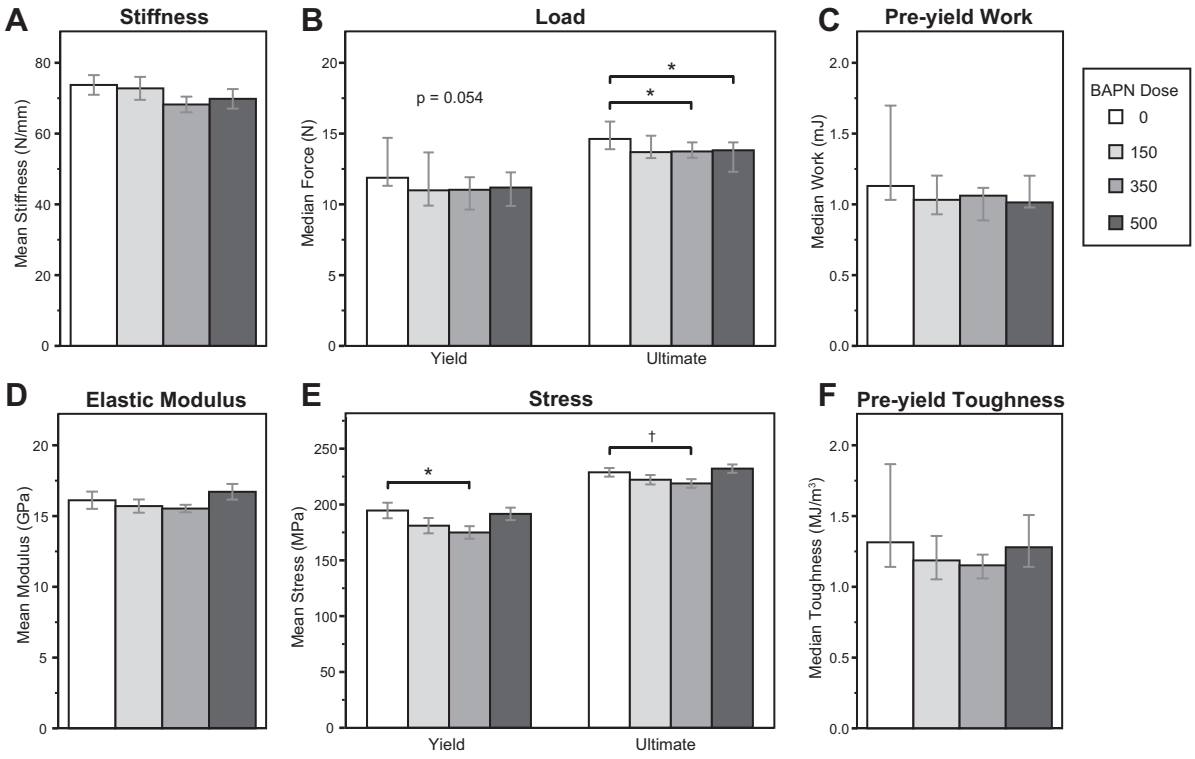

Fig. 5. Whole-bone (*A–C*) and tissue level (*D–F*) mechanical properties measured by four-point bending of the tibia. Ultimate strength (*B*) was significantly reduced by BAPN with significant decreases detected for the 350 and 500 mg/kg groups. Yield strength (*B*) showed the same trend. Yield and ultimate stress (E) were significantly reduced by BAPN. Specific group differences were found between the 0 and 350 mg/kg doses. A marginally significant effect of BAPN on pre-yield toughness (*F*) was observed. No significant differences were detected for stiffness (*A*), pre-yield work (*C*), or modulus (*D*). $^*p < 0.05$, $\dagger p < 0.10$.

$p = 0.038$) and ultimate (ANOVA, $p = 0.044$) stress (Fig. 5*E*). The greatest reductions were not at the highest dose but at the intermediate 350mg/kg dose. An effect of BAPN on pre-yield toughness was marginally significant (Fig. 5*F*, $p = 0.086$). The majority of bones, including controls, sustained significant deformation (>1 mm), necessitating test termination without a defined fracture point and precluding the collection of failure load, failure deformation, and work to fracture data.

Pyridinoline cross-links and cross-link maturity are regressors of bone strength and toughness

The mature/immature cross-link ratio of HP/(DHLNL + HLNL) was the strongest regressor of instability fracture toughness ($r^2 = 0.208$, $p < 0.05$), whereas quantities of mature pyridinoline cross-links were significant positive regressors of tissue strength (LP $r^2 = 0.159$, $p = 0.014$; HP $r^2 = 0.112$, $p < 0.05$) (Table 2).

Table 2. Linear Regression of Mechanics and Cross-Linking

R^2 linear regression	$K_{C.Max}$	$K_{C.Inst}$	Yield stress	Ultimate stress	Pre-yield toughness
Pyrrole (fit using sq.)				0.068	
HP	0.073	0.073	0.089^	0.112*	0.069
LP			0.152*	0.159*	0.118*
HLNL		0.095(–)			
PEN (fit using log)	0.147	0.157^			
HP + LP	0.057	0.065	0.106*	0.128*	0.082
HP + LP + Pyrrole				0.12*	
(HP + LP)/(DHLNL + HLNL)	0.120	0.196^		0.067	
HP/(DHLNL + HLNL)	0.126	0.208*		0.052	
HP/DHLNL		0.172^			
(HP + LP)/DHLNL		0.162^			
LP/HLNL		0.145	0.059	0.055	0.050
Pyrroles/pyridinolines	0.081(–)	0.133(–)			

$R^2 < 0.05$ not shown for clarity. TMD, DHLNL, (DHLNL + HLNL), and modulus had $R^2 < 0.05$ for all metrics and are not shown.
$^*p < 0.05$, $^p < 0.10$; (–) indicates negative relationship. Pre-yield toughness fit using inverse transform (signs corrected to reflect raw data relationship).

Additional ratios reflecting cross-link maturity were marginally significant regressors of $K_{C.Inst}$. Pyridinoline cross-links had significant explanatory power both individually (HP and LP) and summed (HP + LP) for bone strength. No models found TMD to be a significant factor in explaining mechanical properties.

Raman spectroscopy detects localized effects of BAPN treatment on new tissue as increases in the ~1660/1683 ratio

Calcein images were referenced to classify each site of Raman collection as new or preexisting tissue (Supplemental Fig. S1). The cross-linking ratio (Fig. 6*C*) was significantly increased in new BAPN-treated bone compared with newly formed control bone. Within new (treated) tissue, BAPN treatment did not have significant effects on mineral measures (phosphate content or carbonate substitution) (Fig. 6*A, B*). Significant differences between new (treated) and old (preexisting normal) tissues were identified for all Raman measures in all groups, with older tissue having significantly greater mineral/matrix, carbonate/phosphate, and matrix maturity ratio measures than newly formed tissues (Fig. 6*A–C*). Notably, when data were averaged based on cortical location alone (ignoring calcein labels and averaging within mid-cortical and endocortical sites), BAPN's impact on cross-link maturity was masked (Table 3). As was the case for bone, cell matrix 1660/1683 ratio was significantly increased by BAPN treatment (Fig. 6*C*).

Table 3. Comparison of Site-Specific Analyses of Raman Bone Measurements

	Repeated measures 2-way ANOVA		ANOVA (within new tissue)
Factor	Age (calcein label)	BAPN	BAPN
1660/1683	$p < 0.001$	$p = 0.002$	$p = 0.001$
1660/870	$p = 0.001$	$p = 0.396$	$p = 0.266$
1683/870	$p = 0.004$	$p = 0.587$	$p = 0.529$
958/1002	$p < 0.0001$	$p = 0.415$	$p = 0.546$
1070/958	$p < 0.0001$	$p = 0.299$	$p = 0.610$
	Endo versus mid-cortical		
1660/1683	$p < 0.001$	$p = 0.392$	
1660/870	$p = 0.005$	$p = 0.971$	
1683/870	$p = 0.040$	$p = 0.959$	
958/1002	$p = 0.091$	$p = 0.895$	
1070/958	$p = 0.760$	$p = 0.108$	

Raman spectra were averaged for new and preexisting tissue within each bone first based on calcein labeling and then using a broad definition of mid-cortical (old) versus endocortical (new) bone.

Discussion

The toughness of bone stems largely from the properties of its polymeric organic matrix. Covalent collagen cross-links are responsible for stabilizing this fibrillar network. It has long been understood that the inhibition of enzymatic cross-linking results in a reduction in bone strength,[1,15,43] but the degree to which cross-links are capable of directly contributing to bone mechanics, particularly fracture toughness, is unknown. To our knowledge, this is the first report to measure the impact of collagen cross-linking on bone fracture toughness. We found a significant reduction in directly measured bone fracture toughness as a result of cross-link inhibition (Fig. 4). Reduced fracture toughness was accompanied by a significant reduction in tibia whole-bone strength (ultimate load) and estimated material level properties (yield stress and ultimate stress) for the intermediate BAPN dose (Fig. 5).

Ratios reflecting relative cross-link maturity were significant explanatory variables of fracture toughness, whereas quantities of mature pyridinoline cross-links were significant regressors of tissue strength (Table 2). There was a stronger association between pyridinoline content and strength and toughness than pyrrole content (Table 2). The pyrrole colorimetric assay is a

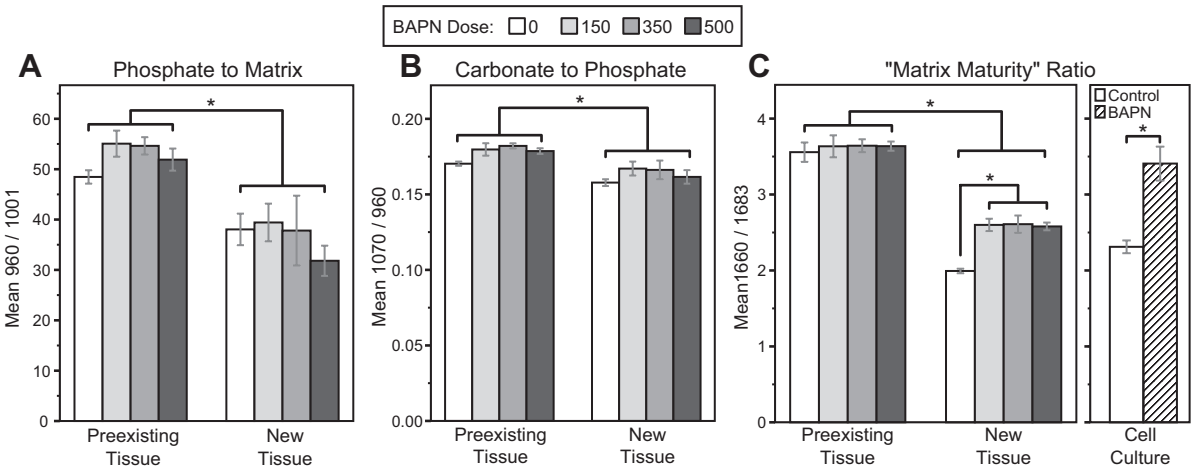

Fig. 6. Raman spectroscopy measures. New tissues had significantly lower mineral:matrix (*A*), carbonate:phosphate (*B*), and matrix maturity (1660/1683) ratio (*C*) compared with older, preexisting tissues. Within new treated tissue, BAPN did not have significant effects on mineral measures but significantly increased the matrix maturity ratio (*C*). MC3T3-E1 cell culture matrix cultured with BAPN had increased 1660/1683 compared with control cultures (*C*). $^{*}p < 0.05$.

noisier measure than the HPLC quantification of pyridinoline, and it is possible this variability reduced our ability to detect significance in pyrrole differences and regressions. The plentiful immature cross-links failed to correlate with bone strength, whereas reductions in the smaller fraction of mature cross-links resulted in measurable losses of tissue strength and fracture toughness. These correlations strengthen the argument that trivalent cross-links play a greater role than the divalent cross-links in stabilizing the organic matrix of bone.

BAPN treatment significantly reduced maximum load toughness but not instability toughness (Fig. 4). This may be explained by the greater variance in the measurement of $K_{C.Inst}$ than $K_{C.Max}$, reducing its power to statistically detect differences between groups. Yet, $K_{C.Inst}$ regressed more strongly than $K_{C.Max}$ with cross-link profile and with measures of bone strength determined from whole-bone bending (Table 2). $K_{C.Inst}$ includes contributions of both crack initiation and stable crack growth and is considered a better single-point fracture toughness estimate than $K_{C.Max}$.[34] The significant association between cross-link maturity and $K_{C.Inst}$ but not $K_{C.Max}$ suggests the possibility that having more mature cross-links relative to immature is supportive of stable crack growth.

We originally hypothesized that a decrease in collagen cross-linking with concomitant decreases in mechanical properties would occur as BAPN dose increased. However, mechanical properties were reduced most significantly at the intermediate (350 mg/kg) rather than highest (500 mg/kg) BAPN dose (Figs. 4 and 5). Others have observed similar discontinuities in BAPN dose effects in vascular tissues.[44] BAPN does not alter existing cross-links. Thus, at the end of the experiment, each mouse is a hybrid of normal and cross-link–deficient tissues in proportions determined by the rates of tissue apposition and removal. The dose-dependent reduction in weight gain and bone cortical area with BAPN treatment (Table 1) support there being less new (BAPN-treated) cortical tissue formed at the highest BAPN dose compared with the other groups. It is also possible that BAPN increased osteoclast number or activity, contributing to reduced bone size.[45] Regardless of the cellular mechanism, the lack of effect on strength and toughness at the highest BAPN dose could be explained by a reduction or change in distribution of the cross-link–deficient tissue. The potential for a volume averaging of preexisting and experimentally treated tissue to influence experimental measurements is an often overlooked confounding factor with broad implications in skeletal research.

The HPLC quantification of cross-links from bulk tissue, while allowing for specific measurement of the full cross-link profile, reflects a volume averaging of preexisting and normal tissue. To address this issue, Raman spectroscopy was used to explore the spatial effect of BAPN treatment on matrix cross-linking and composition. Raman revealed a localized increase in the matrix maturity ratio (1660/1683 cm^{-1}) with LOX inhibition, as well as a strong effect of relative tissue age on both mineral and matrix maturity measures (Fig. 6). It is worth noting that the interpretation of the ~1660/1683 cm^{-1} ratio is still controversial.[27,46] Although the ratio was first reported to correspond to the nonreducible/reducible cross-link ratio using FTIR[47] and has since been widely employed in both the FTIR and Raman spectroscopy literature, it is not a direct measurement of cross-link content. Two component bands of Amide I near 1660 and 1683 cm^{-1} represent different secondary structures of collagen. Thus, the ratio can be changed by factors other than aging, such as mechanical damage,[48] ionizing radiation,[41,49] exercise,[50] and dehydration of bone,[51] all of which cause changes in collagen secondary structure.

Because the ~1660/1683 cm^{-1} ratio is sensitive to tissue age, this sensitivity can overshadow the effects from BAPN treatment if areas of new tissue formation are assumed from cortical location alone. This is illustrated by a lack of significance when tissue measures were averaged by cortical location rather than by calcein labeling (Table 3). Because of the magnitude of the increase in the ratio we observed with increasing tissue age (older preexisting tissue compared with new control tissue, Fig. 6*C*), it is possible the increase in 1660/1683 cm^{-1} observed in newly formed BAPN-treated tissue may be masked at time points later than we examined, after tissue maturation.

The Raman ~1660/1683 cm^{-1} ratio was increased both by BAPN treatment and with relative tissue age, yet direct quantification by HPLC found significant reductions in mature cross-links and relative cross-link maturity. An increase in the spectroscopic matrix maturity ratio was similarly observed by FTIR after BAPN ingestion in rats, but the increase was attributed to disproportionate decreases of HPLC-measured nonreducible and reducible cross-link concentrations in BAPN-treated specimens compared with controls.[27] Combined, these results demonstrate that an increase in the 1660/1683 cm^{-1} ratio does not directly indicate an increase in the number of mature cross-links, highlighting the nonquantitative nature of this measure and the necessity for care in its interpretation. Although the ratio is not an absolute quantification of cross-link maturity, the present results highlight an ability of Raman spectroscopy to detect localized matrix differences attributable to cross-linking deficiencies, if carefully controlling for treatment history and relative age of the tissue.

Our model of BAPN treatment resulted in a significant reduction in mature enzymatic cross-links, but with a greater reduction of LP than HP (Fig. 2), in agreement with others' results.[27] However, we did not observe any change in immature cross-links with BAPN treatment, resulting in a reduced ratio of mature to immature cross-links (Fig. 3). The reduced ratio of mature to immature cross-links from BAPN treatment does not appear to reflect a general perturbation of tissue maturation. Raman measurements showed mineralization in the newly formed BAPN-treated tissue to be equivalent to controls, and BAPN actually increased the ~1660/1683 cm^{-1} ratio in new bone (Fig. 6), an observation typically associated with an increase in matrix maturity.

The maturation of the divalent cross-links to the trivalent cross-link forms is dependent on the presence of another (hydroxy) lysyl-aldehyde, created by LOX activity. It is interesting to consider that we may have developed a mild lathyrism model capable of just enough inhibition to limit the formation of trivalent cross-links, while allowing normal levels of immature cross-linking to develop. It is also possible that metabolism and clearance of the inhibitor permits LOX activity, and thereby immature cross-linking, to recover between the daily BAPN injections.

Our results show correlations between cross-link profile and mechanical properties, but alterations in cross-link profile may alter the response of osteoblasts and osteoclasts, initiating a cell-mediated cascade of changes to tissue quality.[42,45,52,53] The inhibition of cross-linking may affect bone composition and mechanical properties indirectly through these changes in addition to a direct mechanical contribution to matrix stability. However, we did not detect any matrix alterations outside of cross-link profile to explain the mechanical effects of BAPN treatment (Fig. 6). The effects of BAPN treatment on bone mineralization are mixed.[27,28,30,54] TMD is typically expected to be a primary determinant of bone stiffness, but mean TMD, like stiffness, was not significantly changed with cross-link inhibition in this model and was not a significant correlate of any mechanical

property. Cortical TMD at the tibia standard site was more variable with BAPN treatment (Fig. 1), but the BAPN reduction of bone size and the differences in phosphate/matrix and carbonate/phosphate observed with tissue age, but not BAPN treatment, suggest this increased TMD variability is attributable to variability in the volume fractions of new and old tissue rather than effects of BAPN on new tissue mineralization. It is possible that BAPN treatment caused unobserved changes to mineral composition or tissue structure that contributed to the decreases in material strength and fracture toughness.

Considering the possibility that BAPN treatment might promote differences in collagen fibril deposition or organization to indirectly alter mechanical properties, we observed the embedded tibia cross sections with a cross-polarized light microscope to assess collagen alignment via its natural birefringence using the light intensity ($I_{Brightfield}/I_{Darkfield}$) ratio.[55] We observed collagen alignment differences between anatomical locations as others have observed,[56] but there was no indication of BAPN having any impact on collagen alignment within areas of new bone formation (data not shown). Others have observed differences in fibril size distribution with BAPN.[57,58] Perhaps there is a dosage effect of BAPN on fibril morphology, which is responsible for the dose-specific mechanical results observed in our study.

The relationships between cross-linking and mechanical properties were observed in young mice, demonstrating the sufficiency of cross-link changes to affect bone quality in this population at least. Because only young mice were included in this experiment, further study exploring the interaction of cross-linking perturbations with aging and disease-associated changes in bone quality, such as increased mineralization and damage accumulation, is needed to extend these findings to an older population. However, we expect that collagen cross-links similarly contribute to the fracture toughness of adult tissues, as the inclusion of specific mature enzymatic collagen cross-link measures significantly improved regression models predicting strength, stiffness, and ultimate strain in human adult cancellous bone.[59]

Our study reveals that spatially localized effects of short-term BAPN cross-link inhibition can significantly affect whole-bone collagen cross-link profile and reduce both fracture toughness and bone strength. The specific reduction of pyridinoline cross-links and the associated decrease in pyridinoline to immature cross-link ratios were associated with a reduction in bone strength and fracture toughness, respectively. Thus, cross-link profile perturbations associated with bone disease may provide insight into bone mechanical quality and fracture risk.

Disclosures

All authors state that they have no conflicts of interest.

Acknowledgments

The authors sincerely thank Simon Robins for his gift of immature cross-link standards and Sidharth Bhandari for his technical assistance. Research reported in this publication was supported by the National Institute of Arthritis and Musculoskeletal and Skin Diseases of the National Institutes of Health under award number R01 AR056657 (MDM) and by the National Institute of Dental and Craniofacial Research of the National Institutes of Health under award number T32 DE007057 (EM). The content is solely the responsibility of the authors and does not necessarily represent the official views of the National Institutes of Health.

Authors' roles: Study design: EM and DK. Study conduct: EM. Data collection: EM and BG. Data analysis: EM and BG. Data interpretation: EM, BG, MM, and DK. Drafting manuscript: EM. Revising manuscript content: EM and DK. Approving final version of manuscript: EM, BG, MM, and DK. EM and DK take responsibility for the integrity of the data analysis.

References

1. Saito M, Marumo K. Collagen cross-links as a determinant of bone quality: a possible explanation for bone fragility in aging, osteoporosis, and diabetes mellitus. Osteoporos Int. 2010;21(2):195–214.
2. Donnelly E. Methods for assessing bone quality: a review. Clin Orthop Relat Res. 2010;469(8):2128–38.
3. Viguet-Carrin S, Garnero P, Delmas PD. The role of collagen in bone strength. Osteoporos Int. 2006;17(3):319–36.
4. Burr DB, Turner CH. Biomechanics of bone. In: Favus M, editor. Primer on the metabolic bone diseases and disorders of mineral metabolism. 5th ed. Washington DC: American Society for Bone and Mineral Research; p. 58–64. 2003.
5. Reilly DT, Burstein AH. Review article. The mechanical properties of cortical bone. J Bone Joint Surg Am. 1974;56(5):1001–22.
6. Currey JD. Role of collagen and other organics in the mechanical properties of bone. Osteoporos Int. 2003;14(Suppl 5):S29–36.
7. Zioupos P. Ageing human bone: factors affecting its biomechanical properties and the role of collagen. J Biomater Appl. 2001;15(3):187–229.
8. Wang X, Shen X, Li X, Agrawal CM. Age-related changes in the collagen network and toughness of bone. Bone. 2002;31(1):1–7.
9. Uzel SGM, Buehler MJ. Molecular structure, mechanical behavior and failure mechanism of the C-terminal cross-link domain in type I collagen. J Mech Behav Biomed Mater. 2011;4:153–61.
10. Robins S. Fibrillogenesis and maturation of collagens. In: Seibel MJ, Robins SP, Bilezikian JP, editors. Dynamics of bone and cartilage metabolism. 2nd ed. Burlington, MA: Academic Press; 2006. p.41–53.
11. Robins SP, Brady JD. Collagen cross-linking and metabolism. In: Bilezikian JP, Raisz LG, Martin TJ, editors. Principles of bone biology. 3rd ed. San Diego: Academic Press; 2008. p.319–4.
12. Eyre DR, Wu J-J. Collagen cross-links. Top Curr Chem. 2005;247:207–29.
13. Hanson DA, Eyre DR. Molecular site specificity of pyridinoline and pyrrole cross-links in type I collagen of human bone. J Biol Chem. 1996;271(43):26508–16.
14. Eyre DR, Weis MA, Wu J-J. Advances in collagen cross-link analysis. Methods. 2008;45(1):65–74.
15. Knott L, Bailey AJ. Collagen cross-links in mineralizing tissues: a review of their chemistry, function, and clinical relevance. Bone. 1998;22(3):181–7.
16. Robins SP. The separation of cross-linking components from collagen. In: Hall DA, editor. The methodology of connective tissue research. Oxford: Joynson-Bruvvers; 1976. p.37–52.
17. Bailey AJ, Sims TJ, Avery NC, Halligan EP. Non-enzymic glycation of fibrous collagen: reaction products of glucose and ribose. Biochem J. 1995;305(Pt 2):385–90.
18. Smith-Mungo LI, Kagan HM. Lysyl oxidase: properties, regulation and multiple functions in biology. Matrix Biol. 1998;16(7):387–98.
19. Paschalis EP, Shane E, Lyritis G, Skarantavos G, Mendelsohn R, Boskey AL. Bone fragility and collagen cross-links. J Bone Miner Res. 2004;19(12):2000–4.
20. Knott L, Whitehead CC, Fleming RH, Bailey AJ. Biochemical changes in the collagenous matrix of osteoporotic avian bone. Biochem J. 1995;310(Pt 3):1045–51.
21. Saito M, Fujii K, Mori Y, Marumo K. Role of collagen enzymatic and glycation induced cross-links as a determinant of bone quality in spontaneously diabetic WBN/Kob rats. Osteoporos Int. 2006;17(10):1514–23.

22. Burr DB. Bone material properties and mineral matrix contributions to fracture risk or age in women and men. J Musculoskelet Neuronal Interact. 2002;2(3):201–4.
23. Viguet-Carrin S, Roux JP, Arlot ME, et al. Contribution of the advanced glycation end product pentosidine and of maturation of type I collagen to compressive biomechanical properties of human lumbar vertebrae. Bone. 2006;39(5):1073–9.
24. Garnero P, Borel O, Gineyts E, et al. Extracellular post-translational modifications of collagen are major determinants of biomechanical properties of fetal bovine cortical bone. Bone. 2006;38(3):300–9.
25. Mccallum HM. Experimental lathyrism in mice. J Pathol Bacteriol. 1965;89:625–36.
26. Chvapil M, Misiorowski R, Eskelson C. On the mechanisms of beta-aminopropionitrile toxicity. J Surg Res. 1981;31(2):151–5.
27. Paschalis EP, Tatakis DN, Robins S, et al. Lathyrism-induced alterations in collagen cross-links influence the mechanical properties of bone material without affecting the mineral. Bone. 2011;49(6):1232–41.
28. Lees S, Eyre DR, Barnard SM. BAPN dose dependence of mature crosslinking in bone matrix collagen of rabbit compact bone: corresponding variation of sonic velocity and equatorial diffraction spacing. Connect Tissue Res. 1990;24(2):95–105.
29. Kohn RR, Leash AM. Long-term lathyrogen administration to rats, with special reference to aging. Exp Mol Pathol. 1967;7(3):354–61.
30. Di Cesare PE, Nimni ME, Yazdi M, Cheung DT. Effects of lathyritic drugs and lathyritic demineralized bone matrix on induced and sustained osteogenesis. J Orthop Res. 1994;12(3):395–402.
31. Lees S, Hanson D, Page E, Mook H. Comparison of dosage-dependent effects of beta-aminopropionitrile, sodium fluoride, and hydrocortisone on selected physical properties of cortical bone. J Bone Miner Res. 1994;9(9):1377–89.
32. Bouxsein ML, Boyd SK, Christiansen BA, Guldberg RE, Jepsen KJ, Müller R. Guidelines for assessment of bone microstructure in rodents using micro-computed tomography. J Bone Miner Res. 2010; 25(7):1468–86.
33. Wallace JM, Golcuk K, Morris MD, Kohn DH. Inbred strain-specific response to biglycan deficiency in the cortical bone of C57BL6/129 and C3H/He mice. J Bone Miner Res. 2009;24(6):1002–12.
34. Ritchie RO, Koester KJ, Ionova S, Yao W, Lane NE, Ager JW. Measurement of the toughness of bone: a tutorial with special reference to small animal studies. Bone. 2008;43(5):798–812.
35. Roberts HC, Knott L, Avery NC, Cox TM, Evans MJ, Hayman AR. Altered collagen in tartrate-resistant acid phosphatase (TRAP)-deficient mice: a role for TRAP in bone collagen metabolism. Calcif Tissue Int. 2007; 80(6):400–10.
36. Brown S, Worsfold M, Sharp C. Microplate assay for the measurement of hydroxyproline in acid-hydrolyzed tissue samples. Biotechniques. 2001;30(1):38–40 42.
37. Gineyts E, Borel O, Chapurlat R, Garnero P. Quantification of immature and mature collagen crosslinks by liquid chromatography-electrospray ionization mass spectrometry in connective tissues. J Chromatogr B Analyt Technol Biomed Life Sci. 2010;878(19):1449–54.
38. Spacek P, Adam M. HPLC method for pentosidine determination in urine, serum, and tissues as a marker of glycation and oxidation loading of the organism. J Liq Chromatogr Relat Technol. 2002; 25(12):1807–20.
39. Słowik-Zyłka D, Safranow K, Dziedziejko V, Bukowska H, Ciechanowski K, Chlubek D. A sensitive and specific HPLC method for the determination of total pentosidine concentration in plasma. J Biochem Biophys Methods. 2004;61(3):313–29.
40. Henle T, Schwarzenbolz U, Klostermeyer H. Detection and quantification of pentosidine in foods. Zeitschrift für Leb und -forsch A. 1997;204(2):95–8.
41. Gong B, Oest ME, Mann KA, Damron TA, Morris MD. Raman spectroscopy demonstrates prolonged alteration of bone chemical composition following extremity localized irradiation. Bone. 2013; 57(1):252–8.
42. Fernandes H, Dechering K, Van Someren E, et al. The role of collagen crosslinking in differentiation of human mesenchymal stem cells and MC3T3-E1 cells. Tissue Eng Part A. 2009;15(12):3857–67.
43. Oxlund H, Barckman M, Ørtoft G, Andreassen T, Ortoft G. Reduced concentrations of collagen cross-links are associated with reduced strength of bone. Bone. 1995;17(4 Suppl):365S–71S.
44. Li J, Li H, Wang L, Zhang L, Jing Z. Comparison of beta-aminopropionitrile-induced aortic dissection model in rats by different administration and dosage. Vascular. 2013;21(5):287–92.
45. El Rouby DH, Bashir MH, Korany NS. Ultrastructural and histomorphometric alterations of rat jaw bones after experimental induction of lathyrism. Arch Oral Biol. 2008;53(10):916–23.
46. Farlay D, Duclos M-E, Gineyts E, et al. The ratio 1660/1690 cm(-1) measured by infrared microspectroscopy is not specific of enzymatic collagen cross-links in bone tissue. PLoS One. 2011;6(12):e28736.
47. Paschalis EP, Verdelis K, Doty SB, Boskey AL, Mendelsohn R, Yamauchi M. Spectroscopic characterization of collagen cross-links in bone. J Bone Miner Res. 2001;16(10):1821–8.
48. Carden A, Rajachar RM, Morris MD, Kohn DH. Ultrastructural changes accompanying the mechanical deformation of bone tissue: a Raman imaging study. Calcif Tissue Int. 2003;72(2):166–75.
49. Barth HD, Zimmermann EA, Schaible E, Tang SY, Alliston T, Ritchie RO. Characterization of the effects of x-ray irradiation on the hierarchical structure and mechanical properties of human cortical bone. Biomaterials. 2011;32(34):8892–904.
50. Kohn DH, Sahar ND, Wallace JM, Golcuk K, Morris MD. Exercise alters mineral and matrix composition in the absence of adding new bone. Cells Tissues Organs. 2009;189(1–4):33–7.
51. Zhu P, Xu J, Sahar N, Morris MD, Kohn DH, Ramamoorthy A. Time-resolved dehydration-induced structural changes in an intact bovine cortical bone revealed by solid-state NMR spectroscopy. J Am Chem Soc. 2009;131(47):17064–5.
52. Turecek C, Fratzl-Zelman N, Rumpler M, et al. Collagen cross-linking influences osteoblastic differentiation. Calcif Tissue Int. 2008;82(5): 392–400.
53. Valcourt U, Merle B, Gineyts E, Viguet-Carrin S, Delmas PD, Garnero P. Non-enzymatic glycation of bone collagen modifies osteoclastic activity and differentiation. J Biol Chem. 2007;282(8):5691–703.
54. Rosenquist J, Baylink D, Spengler D. The effect of beta-aminopropionitrile (BAPN) on bone mineralization. Proc Soc Exp Biol Med. 1977;154(2):310–3.
55. Martin RB, Ishida J. The relative effects of collagen fiber orientation, porosity, density, and mineralization on bone strength. J Biomech. 1989;22(5):419–26.
56. Ramasamy JG, Akkus O. Local variations in the micromechanical properties of mouse femur: the involvement of collagen fiber orientation and mineralization. J Biomech. 2007;40(4):910–8.
57. Hong H-H, Pischon N, Santana RB, et al. A role for lysyl oxidase regulation in the control of normal collagen deposition in differentiating osteoblast cultures. J Cell Physiol. 2004;200(1): 53–62.
58. Gerstenfeld LC, Riva A, Hodgens K, Eyre DR, Landis WJ. Post-translational control of collagen fibrillogenesis in mineralizing cultures of chick osteoblasts. J Bone Miner Res. 1993;8(9): 1031–43.
59. Banse X, Sims TJ, Bailey AJ. Mechanical properties of adult vertebral cancellous bone: correlation with collagen intermolecular cross-links. J Bone Miner Res. 2002;17(9):1621–8.